Applied Thermal Engineering 240 (2024) 122080

Contents lists available at ScienceDirect

Applied Thermal Engineering

journal homepage: www.elsevier.com/locate/apthermeng

Research Paper

Energy and exergy analysis of a novel solar-based system merged with power cycle

Mohamad Abou Houran [a], Abd Alwahed Dagestani [b,h], Tirumala Uday Kumar Nutakki [c], Aliashim Albani [d,*], Ahmad A. Ifseisi [e], Fahid Riaz [f], Fan Peng [g,*]

[a] School of Electrical Engineering, Xi'an Jiaotong University, Xi'an, 710049, China
[b] School of Business, Central South University, Changsha, 410083, China
[c] RAK Research and Innovation Center, American University of Ras Al Khaimah, United Arab Emirates
[d] Faculty of Ocean Engineering Technology and Informatics, Universiti Malaysia Terengganu, 21030, Kuala Nerus, Terengganu, Malaysia
[e] Department of Chemistry, College of Science, King Saud University, P.O. Bo x 2455, Riyadh, 11451, Saudi Arabia
[f] College of Engineering, Abu Dhabi University, Abu Dhabi, United Arab Emirates
[g] Sustainable Management of Natural Resources and Environment Research Group, Faculty of Environment and Labour Safety, Ton Duc Thang University, Ho Chi Minh City, Viet Nam
[h] Faculty of Economics, University of Tishreen, P.O. Box 2230, Lattakia, Syria

ARTICLE INFO

Keywords:
Organic Rankine cycle
Photovoltaic module
Parabolic trough collector
Nuermcial simulation
Exergy
Energy

ABSTRACT

Parabolic Trough Solar Collector (PTC) is a power generation unit that works based on solar energy. This system provides a considerable amount of thermal power but no electrical energy. Hence, the current investigation attempts to boost the outputs of the PTC system by merging this unit with the Photovoltaic (PV) module and Organic Rankine Cycle (ORC). In this regard, the outputs of the conventional PTC system under multiple operating conditions are compared with those of PTC-PV, PTC-ORC, and PTC-PV-ORC systems. These systems are three-dimensionally simulated using the steady-state approach and the influences of variation in the solar flux and concentration ratio on the energy and exergy efficiencies are scrutinized. According to the obtained data, at the base case condition, the overall energy efficiencies of the conventional PTC, PTC-PV, PTC-ORC, and PTC-PV-ORC systems are 42.75%, 47.20%, 13.43%, and 21.46%, respectively. The performance of these systems from the exergy viewpoints is 5.51%, 14.31%, 4.19%, and 13.33%, respectively. Based on the simulations, from the electrical energy and exergy viewpoints, the PTC-PV-ORC system has the highest performance followed by PTC-PV and PTC-ORC systems. Nonetheless, the thermal exergy of the ORC-based systems is remarkably lower than that of single solar units. This study shows the integration of the PTC system with the PV module and ORC boosts the output of this conventional unit.

1. Introduction

These days, due to the intense growth in the human population, energy demand is rising rapidly. Renewable energies are reliable sources that can maintain this essential need. Among various renewable energy sources, solar energy is the most prominent one due to its availability in any location. One of the most functional solar energy units is the Parabolic Trough Collector (PTC). PTC can provide thermal energy by concentrating the solar irradiance on the receiver tube surface [1]. This system consists of a parabolic reflector and a receiver tube that converts solar irradiance into heat [2]. Heretofore, manifold studies are conducted on evaluating the outputs of the PTC system.

The consequence of utilizing a heat shield on the PTC exergy and energy performances is assessed by El-Bakry et al. [3]. According to this scientific work, using a heat shield can enhance the exergy and energy efficiency of the PTC system by around 15.4 % and 14.4 %, respectively. The effect of using an evacuated and non-evacuated receiver tube on the PTC operational performance is poked by Reddy and Ananthsornaraj [4]. It is found that the variation in the first law efficiency of the system by evacuation of the receiver tube is almost negligible.

In addition to these strategies, adding nanoparticles to the operating fluid may positively affect the performance of the solar energy units. Nanomaterials have high thermal conductivity compared to water and oil leading to elevation in heat exchange between the fluid and system [5].

* Corresponding authors.
E-mail addresses: abd_alwahed_dagestani@hotmail.com (A.A. Dagestani), a.albani@umt.edu.my (A. Albani), Pfanxu@gmail.com (F. Peng).

https://doi.org/10.1016/j.applthermaleng.2023.122080
Received 3 April 2023; Received in revised form 22 October 2023; Accepted 20 November 2023
Available online 23 November 2023

Nomenclature

C_p	Heat capacity at a fixed pressure (J/(kg • K))
D	Fluid channel Diameter (m)
$\dot{E}$	Energy rate (W)
$\dot{E}x$	Exergy rate (W)
F	Collector focal length (m)
G_k	Production of kinetic energy in turbulent flow
k	Heat Conduction coefficient (W/(m • K))
P	Operating fluid pressure (kPa)
T	Temperature (K)
W	Width of the collector (m)
$\dot{W}_{el}$	Electrical power (W)

Greeks

μ	Dynamic viscosity (kg/(m • s))
β	Liquid volume fraction
$\varnothing$	Nanofluid mass fraction
κ	Kinetic energy of turbulent flow
$\in$	dissipation rate of turbulent flow
η	Generation unit performance (%)
ρ	ORC operating fluid density (kg/m^3)
σ	Stefan-Boltzmann coefficient (W/(m^2 • K^4))
ε	Glass emissivity
φ	Rim angle (°)

Subscripts

amb	Ambient state
el	Electrical
the	Thermal
r	Base case
g	Glass Cover
s	Solid-state
w	Wind effect

Javidan et al. [6] evaluated the performance of a nanofluid-based PTC system equipped with different fin shapes. The shape of installed fins inside the receiver tube includes square, circle, triangle, and combined square-circle. The outputs of the simulations show that installing square-circular shape fins enhances the thermal output of the system by around 39 %. Moreover, using hybrid TiO_2/Cu nanoparticles in the base fluid boosts the coefficient of heat transfer by approximately 21 %. The influence of adding Al_2O_3 and CuO to the operating fluid on the performance of a PTC system is studied by Farooq et al. [7]. The thermal efficiencies of the PTC system at the mass flow rate of 0.0112 kg/s are computed to be 13.01 % and 13.92 % using Al_2O_3 and CuO, respectively. At the mass flow rate of 0.0224 Kg/s, the thermal outputs of the system are obtained to be 13.1 % and 14.79 % using Al_2O_3 and CuO, respectively. Hence, the CuO-based PTC system is superior to the Al_2O_3-based system from the thermal efficiency viewpoint.

The thermal performance of a nanofluid-based PTC system equipped with internal fins and porous foam is scrutinized by Samiezadeh et al. [8]. The outputs demonstrate that increasing the volume fraction of nanoparticles enhances the thermal output of the system. Moreover, a reduction in solar flux causes an increment in the temperature gradient inside the fluid channel.

It is noteworthy to mention that, using strip inserts [9,10] and turbulators [11] inside the fluid channel have constructive effects on the performances of the nanofluid-based PTC systems. Furthermore, using rotary receiver tubes is one of the novel methods, in improving the performance of PTC systems. The comparison between the thermal performance of a PTC system with rotary and stationery receivers is conducted by Reddy et al. [12]. The experimental data reveals that reduction in the water inlet temperature and elevation in the mass flow rate, boost the thermal output of the PTC system. The thermal performance of the PTC system with receiver rotational velocities of 4 rpm and 2 rpm are computed to be 158 % and 190 %, respectively, higher than that of a system with stationary receiver.

Even though the PTC system can produce thermal energy, it is unable to provide electrical energy for human use. Thus, the combination of the PTC unit with the solar cells can enhance its overall performance. By the installation of a Photovoltaic (PV) module on the absorber layer of the common PTC unit, the renewable-based generation system will produce both thermal and electrical energies.

Soltani et al. [13] studied the thermal and electrical output of a PTC system merged with a PV module and thermoelectric generator. In this mathematical investigation, it is interpreted that the hybrid system can provide 22.7 W electrical power a the solar flux of 998 W/m^2. In addition, the maximum thermal efficiencies of the system are obtained to be around 75 %. Herez et al. [14] evaluated the electrical energy and thermal energy efficiencies of a PTC-PV unit. As reported, increasing the fluid momentum enhances the generated power of the mentioned system. It is deduced that the greatest overall efficiency of the unit is around 82 %.

In another study, Padhy et al. [15]. fabricated a PTC-PV unit and examined the thermal and electrical output of the unit. The obtained data demonstrate the electrical efficiency and temperature difference of the system are 14.93 % and 11.4 °F, respectively. The cost of fabricating this hybrid system is estimated to be Rs. 15,000. Besides, the performances of a PTC-PV unit are evaluated from various viewpoints including energy and exergy by Fu et al. [16]. Based on the outcomes, the optimum electrical performance of the unit is obtained at the solar flux of 900 W/m^2. The value of saved cost, entropy generation, and CO2 emission are found to be 70 USD/month, 23.9 W/m.K, and 804.0 kg/month, respectively, at the optimum operating condition of the system. Additionally, merging PTC systems with power generator systems such as Organic Rankine Cycle (ORC) can boost the overall energy output of the unit and provide electrical energy. ORC is a system consisting of a condenser, a small turbine, a pump, and a heat exchanger that can convert low-grade thermal energy into electrical [17].

The exergy and energy performances of a water heating unit and an ORC subsystem are scrutinized by Aziz et al. [18]. In this etude, the impact of some operating fluids with low critical temperatures on the system performance is investigated. It is concluded that the system with working fluids of R245fa and m-xylene has the highest performance. The energy, exergy, and economic analysis of a PTC system integrated with ORC and partial evaporation Rankine cycle is evaluated by Habibi et al. [19]. Based on the results, the amount of total cost rate, exergy efficiency, and output energy power of the designed system are 228 $/h, 18.6 %, and 782 kW, respectively. The performance of a PTC system combined with ORC and Phase Change Material (PCM) storage is scrutinized by Pourmoghadam et al. [20]. In this evaluation, the impact of using multiple operating fluids including R134a/R245fa, R245fa/R1234yf, and R500/R245fa on the performance of the system is studied. The outputs reveal that the R500/R245fa is the best operating fluid from both energy and exergy performance viewpoints. Moreover, the net present value, payback period, and levelized cost of energy are computed to be 186,622 $, 18 years, and 0.29 $/kWh, respectively. Besides, some researchers combined the PTC system with ORC and electrolyzer to produce hydrogen fuel [21,22].

Based on the research studies, manifold investigations are conducted on the performance of the PTC systems integrated with power systems. Nevertheless, there are various scientific gaps in this field of research. Currently, no investigations are performed on the energy and exergy analysis of the PTC system integrated with both the PV module and ORC.

Besides, there is no comprehensive study on the comparison of different types of hybrid PTC-based systems. Thus, in the present research, the outcomes of conventional PTC systems are compared with those of PTC-ORC, PTC-PV, and PTC-PV-ORC systems. In this order, the PTC system is designed three-dimensionally by considering all layers including glass cover, air gap, solar cells (PV module), absorber layer, and fluid channel. Furthermore, the PTC unit operating fluid is VP-1 and the working fluid of ORC is R407c. In the following, the details of the present study are presented.

2. Numerical modeling

In this study, the energy and exergy performance of all PTC, PTC-PV, PTC-ORC, and PTC-PV-ORC systems are scrutinized. For this purpose, initially, the details of the simulation of the PTC system are presented. Henceforth, the specifications of the ORC are presented.

2.1. PTC and PTC-PV system

To obtain accurate numerical outputs, both PTC and PTC-PV systems are designed and simulated three-dimensionally. A schematic view of the implemented PTC-PV generation unit is pictured in Fig. 1. As noticed in the mentioned figure, the PTC-PV system consists of various layers including a glass envelope, air spacing zone, PV module, absorber, and fluid channel. It should be noted that the only difference between the PTC and PTC-PV renewable systems is the lack of the PV cell on the PTC unit. Moreover, to exploit the consequence of reflector geometry on the mentioned system performance, the solar flux dispensation on the surface of the receiver tube is calculated and imposed.

An open-source Soltrace software is utilized to compute the distribution of solar irradiance on the receiver. In this software, by defining the characteristics of the receiver tube and the reflector, the solar irradiance distribution on the receiver can be computed. In these simulations, PV module absorptivity and the transmissivity of the glass coating are considered to be 0.95 and 0.97, respectively. Moreover, the collector slope error is assumed to be 3 mrad and the collector mirror's specularity error is considered to be 0.5 mrad. The selected values of specularity and slop errors are in line with measurements performed by Wendelin [23]. In the Soltrace software, to obtain the solar flux distribution over the receiver tube, 100 million sun rays are generated and tracked through optical interactions of the PTC system. Furthermore, the desired number of ray intersections is considered to be 1 million.

Also, the dimensions and thermodynamic characteristics of the different parts of the proposed renewable unit are shown in Tables 1 and 2, respectively.

Regarding the PTC system, the solar irradiance dispensation over the absorber zone is extremely dependent on the reflector size. In the PTC systems, the equation of the reflector can be proposed as [26]:

$$x^2 = 4Fy \tag{1}$$

Also, the focal length of the reflector, where the tube is installed can be calculated by [26]:

Table 1
Thermodynamic characteristics of the different pieces of the introduced generation units [24,25].

Components	Material density (kg/m^3)	Heat conduction coefficient (W/(m • K))	Specific heat capacity at fixed pressure (J/(kg • K))
Glass coating	2221	0.765	829.9
PV cell layer	2331	148.1	701
Air spacing zone	1200	0.20	1250
Absorber zone	8960	401.1	385.1

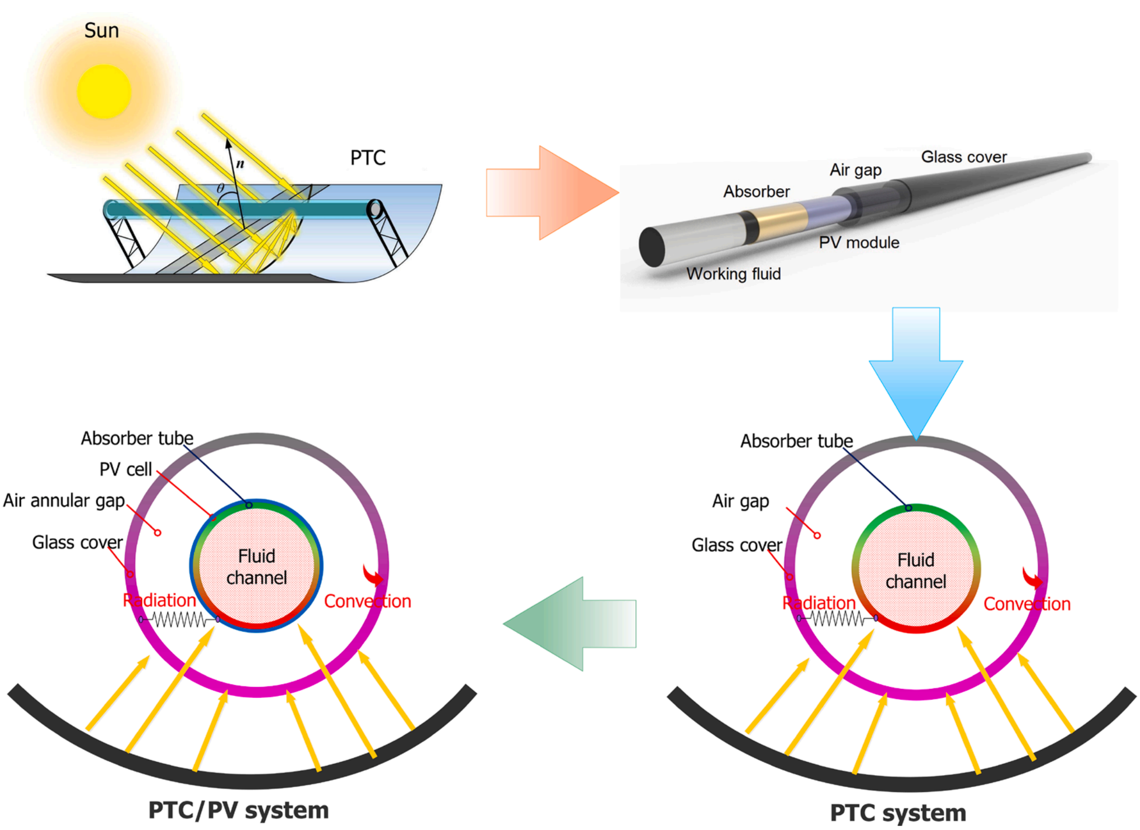

Fig. 1. The 3D and 2D views of the introduced PTC-PV generation unit.

Table 2
Geometrical properties of the different parts of the introduced generation units.

Parts	Value
Glass cover thickness (mm)	3.2
Air spacing zone thickness (mm)	20
PV cell thickness (mm)	0.301
Absorber zone thickness (mm)	3.0
Diameter of the fluid channel (mm)	38
Length of the reflector and receiver tube (m)	5
Aperture wide of reflector (m)	8

$$F = \frac{W}{4\tan(\varphi/2)} \tag{2}$$

in this equation, W and φ are aperture wide and the rim angle of the reflector is considered to be 80°. Moreover, the concentration ratio of the system can be determined as [26]:

$$C = \frac{W}{d} \tag{3}$$

where d is the absorber zone diameter. The concentration ratio of the renewable-based generation unit is considered to be variable in the range of 25 to 45.

2.2. ORC

In the present systems, the ORC consists of different components including a small turbine, a condenser, a pump, and a heat exchanger. In this hybrid unit, the R407c is chosen as the operating fluid of the ORC based on the findings of Singh and Mishra [27]. According to this research paper, the R407c is one of the best fluids for deriving the ORC.

In both the PTC-ORC and PTC-PV-ORC systems, the needed thermal energy of the ORC is maintained by the PTC system. In the heat exchanger, the cold R407c absorbs the thermal energy of the hot VP-1 and transfers it from liquid to gas state. Henceforth, the R407c moves toward the turbine, and the VP-1 moves toward the inlet of the PTC system. In the ORC, the R407c drives the turbine and produces electrical energy, afterward, by a reduction in the pressure of the gas, the R407c moves toward the condenser to lose its heat and change to the liquid state. Finally, liquid R407c enters the pump to get energy for circulation in the cycle. In Fig. 2, a schematic view of the coupled PTC-ORC unit is presented.

2.3. Boundary condition

In this section, the applied boundary conditions on the designed systems are explained. The "inlet mass flow rate" boundary condition is considered at the inlet position of the channel to simulate the working fluid within the tube. In this type of boundary condition, both the mass flow rate and temperature of the working fluid can be clarified. Moreover, at the outlet of the tube, the "pressure outlet" condition is imposed. In this case, the amount of gage pressure at the outlet of the channel is considered to be zero.

The heat generation condition is considered for the PV module, to model the process of solar irradiance absorption in the system. It is noteworthy to mention that the solar flux distribution is imposed on the tube using a User Defined Function (UDF).

On top of that, for simulation of the heat loss phenomenon of the collector receiver, the "wall" with "mixed heat transfer" is imposed for the surface of the glass cover. In this boundary condition, by considering the sky temperature and convection heat transfer coefficient, both convection and radiation mechanisms can be simulated. The convective coefficient and sky temperature are the function of ambient temperature and wind speed respectively. These values are computed using the following equations [28,29]:

$$h_w = V_w^{0.58} d_g^{-0.42} \tag{4}$$

$$T_{sky} = 0.0522 T_{amb}^{1.5} \tag{5}$$

in these equations, V_m, d_g, and T_{amb} are wind speed, absorber diameter, and ambient temperature, respectively.

2.4. Governing equations

In the present study, the systems are designed three dimensional and simulated using the steady-state method. By using this approach and considering the working fluid as a turbulent flow, the mass, momentum, and energy balances can be presented as [30]:

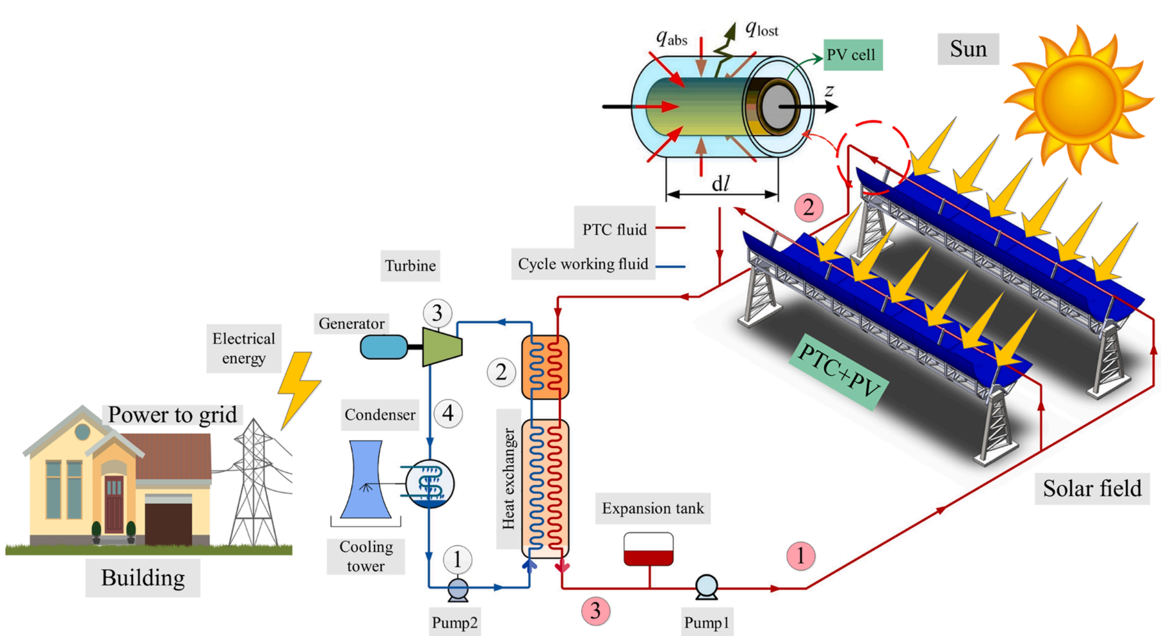

Fig. 2. Schematic diagram of the PTC-ORC hybrid system.

$$\frac{\partial(\rho \overline{u}_i)}{\partial x_i} = 0 \tag{6}$$

$$\frac{\partial(\rho \overline{u}_i \overline{u}_j)}{\partial x_j} = \frac{\partial}{\partial x_j}\left[\mu\left(\frac{\partial \overline{u}_i}{\partial x_j} + \frac{\partial \overline{u}_j}{\partial x_i}\right) - \frac{2}{3}\mu\frac{\partial \overline{u}_i}{\partial x_i}\delta_{ij} - \rho\overline{u_i^{'}u_j^{'}}\right] - \frac{\partial \overline{P}}{\partial x_i} \tag{7}$$

$$\frac{\partial(\rho \overline{u}_j c_p \overline{T})}{\partial x_j} = \left[\mu\left(\frac{\partial \overline{u}_i}{\partial x_j} + \frac{\partial \overline{u}_j}{\partial x_i}\right) - \frac{2}{3}\mu\frac{\partial \overline{u}_i}{\partial x_i}\delta_{ij} - \rho\overline{u_i^{'}u_j^{'}}\right]\frac{\partial \overline{u}_i}{\partial x_i} + \frac{\partial}{\partial x_j}\left(\lambda\frac{\partial \overline{T}}{\partial x_j} + \frac{\mu_t}{\sigma_{h,t}}\frac{\partial(c_p\overline{T})}{\partial x_i}\right) + \overline{u}_j\frac{\partial \overline{P}}{\partial x_j} \tag{8}$$

in these equations, ρ, u, P, and c_p are the density, velocity, pressure, and heat capacity of the working fluid, respectively. In the simulations, due to the turbulence of flow in the channel, the $k-\varepsilon$ model is selected for solving the equations. In this equation, ε is dissipation rate and k is turbulent kinetic energy.

In the above equations, the term $-\rho\overline{u_i^{'}u_j^{'}}$ refers to the Reynolds stress which is computed as [30]:

$$-\rho\overline{u_i^{'}u_j^{'}} = \mu_t\left(\frac{\partial \overline{u}_i}{\partial x_j} + \frac{\partial \overline{u}_j}{\partial x_i}\right) - \frac{2}{3}\left(\rho k + \mu_t\frac{\partial \overline{u}_k}{\partial x_k}\right)\delta_{ij} \tag{9}$$

The value of turbulent kinetic energy can be calculated as [30]:

$$\frac{\partial(\rho k \overline{u}_j)}{\partial x_j} = \frac{\partial}{\partial x_j}\left[\left(\mu + \frac{\mu_t}{\sigma_k}\right)\frac{\partial k}{\partial x_j}\right] + G_k - \rho\varepsilon \tag{10}$$

where,

$$G_k = -\rho\overline{u_i^{'}u_j^{'}}\frac{\partial \overline{u}_j}{\partial x_i} = \mu_t S^2 \tag{11}$$

$$\mu_t = \rho C_\mu \frac{k^2}{\varepsilon} \tag{12}$$

$$S \equiv \sqrt{2S_{ij}S_{ji}} \tag{13}$$

in these equations, G_k is turbulent kinetic energy production, μ_t is eddy viscosity, S donates the linear deformation of a fluid element, and σ_k is a constant value equal to 1.

Furthermore, the value of the dissipation rate can be obtained as [30]:

$$\frac{\partial(\rho\varepsilon \overline{u}_j)}{\partial x_j} = \frac{\partial}{\partial x_j}\left[\left(\mu + \frac{\mu_t}{\sigma_\varepsilon}\right)\frac{\partial \varepsilon}{\partial x_j}\right] + \rho\left(max\left[0.43, \frac{S\frac{k}{\varepsilon}}{S\frac{k}{\varepsilon} + 5}\right]\right)S\varepsilon - \rho C_1\frac{\varepsilon^2}{k + \sqrt{\nu\varepsilon}} \tag{14}$$

in the above equation, the constants of C_1 and σ_ε considered to be 1.9 and 1.2, respectively.

Moreover, some assumptions are made to attenuate the simulations. The suppositions are as follows:

- The thermal properties of the pieces for the PTC-PV and PTC generation systems are considered to be constant versus temperature variation.
- The sky is considered a black body [31].
- The velocity distribution at the receiver tube inlet is supposed to be uniform.
- The solar flux dispensation along the length of the tube is constant.
- The turbine efficiency is considered to be 75 % [32,33].
- The final temperature of the R407c, exiting the heat exchanger is considered to be 6 °C lower than the inlet temperature of the VP-1 to this component.

The VP-1 properties are highly temperature-dependent. In order to calculate the density, thermal conductivity, and heat capacity of the fluid, the following equations can be used [34]:

$$\rho = 1.4386 \times 10^3 - 1.8711T + 2.273 \times 10^{-3}T^2 - 2.3793 \times 10^{-6}T^3 \tag{15}$$

$$\lambda = 0.14644 + 2.0353 \times 10^{-5}T - 1.9367 \times 10^{-7}T^2 + 1.0614 \times 10^{-11}T^3 \tag{16}$$

$$C_p = 2.125 \times 10^3 - 11.017T + 0.049862T^2 - 7.7663 \times 10^{-5}T^3 + 4.394 \times 10^{-8}T^4 \tag{17}$$

Nonetheless, for calculating the viscosity of the VP-1, if the temperature is about 285.15–373.15 K, Eq. (18) can be used. But, if the fluid temperature is in the range of 373.15 K to 698.15, Eq. (19) should be used for computing the mentioned property [34].

$$\mu = 3.661 \times 10^2 - 3.0154T + 8.3409 \times 10^{-3}T^2 - 7.723 \times 10^{-6}T^3 \tag{18}$$

$$\mu = 23.165 - 0.1476T + 3.617 \times 10^{-4}T^2 - 3.9844 \times 10^{-7}T^3 + 1.6543 \times 10^{-10}T^4 \tag{19}$$

3. Thermodynamic study

The control volume method is used to investigate the energy and exergy efficiencies of the simulated systems. In the following sections, the energy and exergy analysis of the simulated systems are provided in two distinct sections.

3.1. Energy analysis

Imposing the control volume method, the energy balance of the systems can be presented as:

$$\dot{E}_{sun} = \dot{E}_{el} + \dot{E}_{th} + \dot{E}_{loss} \tag{20}$$

in these equations, $\dot{E}_{sun}$, $\dot{E}_{th}$, $\dot{E}_{el}$, and $\dot{E}_{loss}$ is the rate of received energy by the system from the sun, the output thermal energy rate, the electrical power rate, and the loss energy rate from the generation cascade to the ambient.

The value of $\dot{E}_{sun}$ can be computed as:

$$\dot{E}_{sun} = \dot{G}_{sun} \bullet W \bullet L \tag{21}$$

in the above equation, $\dot{G}_{sun}$ is the solar flux intensity, W is wide, and L represents the length of the reflector. Besides, the electrical energy output of the system can be calculated based on the following equation [35]:

$$\dot{E}_{el} = \eta_{el} \bullet \dot{E}_{sun} \tag{22}$$

here, η_{el} refers to the electrical performance of the solar cells which can be determined as [36]:

$$\eta_{el} = \eta_{sta} \bullet [1 - 0.0045 \bullet (T_{cell} - 298.15)] \tag{23}$$

In this equation, η_{sta} is the solar cell converting performance at the standard situation (it is equal to 15 % in current research) and T_{cell} is the solar cell operating temperature. Moreover, the output thermal power and efficiency of the proposed systems can be obtained as [37]:

$$\dot{E}_{th} = \dot{m} \bullet C_p \bullet |T_{out} - T_{in}| \tag{24}$$

$$\eta_{th} = \frac{\dot{m} \bullet C_p \bullet |T_{out} - T_{in}|}{\dot{E}_{sun}} \tag{25}$$

in the PTC and PTC-PV systems, T_{out} is the outlet temperature of the collector receiver tube and T_{in} is the inlet temperature of the mentioned receiver. While in the PTC-ORC and PTC-PV-ORC systems, T_{out} is the final temperature of the condenser and T_{in} is the outlet temperature of the R407c at the outlet of the turbine.

3.2. Exergy analysis

The exergy balance of the system can be provided as:

$$\dot{E}x_{sun} = \dot{E}x_{el} + \dot{E}x_{th} + \dot{E}x_{loss} \tag{26}$$

in the above equation, $\dot{E}x_{sun}$, $\dot{E}x_{el}$, $\dot{E}x_{th}$, and $\dot{E}x_{loss}$ is the rate of input sun exergy, the rate of electrical output exergy, the thermal output exergy rate of the renewable-based unit, and the exergy loss rate of the systems. In these equations, the rate of input solar exergy can be obtained as [38]:

$$\dot{E}x_{sun} = \dot{E}_{sun} \bullet \left(1 - \frac{T_{amb}}{T_{sun}}\right) \tag{27}$$

in this equation, T_{sun} is sun temperature which is equal to 5800 K. Furthermore, the output electrical exergy power and exergy efficiency of the system can be computed as [35]:

$$\dot{E}x_{el} = \dot{E}_{el} \tag{28}$$

$$\varepsilon_{el} = \frac{\dot{E}x_{el}}{\dot{E}x_{sun}} \tag{29}$$

Finally, the thermal exergy power and efficiency of the systems are calculated according to the following equations [39]:

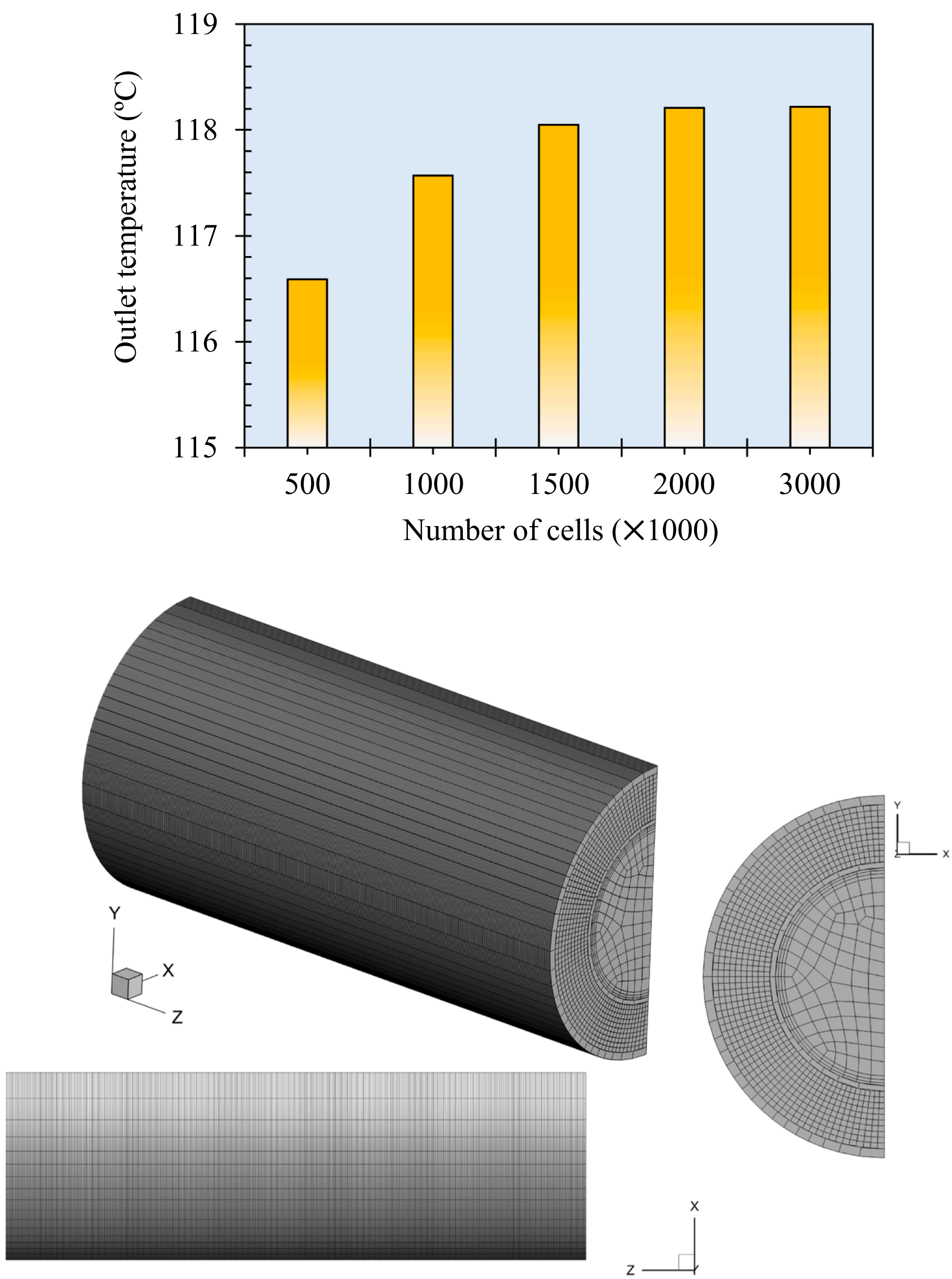

Fig. 3. (a) The variation of operating fluid outlet temperature versus the cell number, (b) lateral view of the generated grid.

$$\dot{E}x_{th} = \dot{m} \bullet [(h_{out} - h_{in}) - T_{amb} \bullet (s_{out} - s_{in})] \quad (30)$$

$$h_{out} - h_{in} = C_p \bullet (T_{out} - T_{in}) \quad (31)$$

$$s_{out} - s_{in} = C_p \bullet \ln\left(\frac{T_{out}}{T_{in}}\right) \quad (32)$$

$$\varepsilon_{th} = \frac{\dot{E}x_{th}}{\dot{E}x_{sun}} \quad (33)$$

4. Grid study and validation

In this section, the impact of mesh density on the obtained data and the validity of the present numerical simulations are investigated. To evaluate the effect of cell number on numerical information, the mentioned PTC-PV hybrid system meshed with 500, 1000, 1500, 2000, and 3000 thousand cells. In Fig. 3, the variation of outlet temperature with the cell number is depicted. As can be seen, by enhancing the mesh density, the variation in the operating fluid outlet temperature is reduced. Based on the output results, the difference between the system with cell numbers of 500 and 1500 thousand cells is around 1.3 %, while this value for the difference between the system with cell numbers of 1500 and 3000 thousand cells is approximately 0.2 %. As a result, the system with a cell number of 1500 thousand is elected for more investigation due to its low time cost and precision.

Moreover, for verification of the obtained solar flux profile from the open-source Soltrace software, the data of the present study are collated with the output information of Mwesigye and Meyer [34]. The dispensation of concentration ratio on the collector receiver tube is depicted in Fig. 4 (a). In order to verify the present simulation, the specifications of the present study are chosen as the same as the study of Mwesigye and Meyer [34]. In this study, the absorber absorptivity, the glass coating transmissivity, the collector slop error, and the mirror specularity error are considered to be 0.96, 0.97, 3 mrad, and 0.5 mrad, respectively. Moreover, the rim angle of the reflector is assumed to be 80°. As shown in Fig. 4 (a), there is a good collusion between the obtained solar irradiance distribution on the receiver tube in the present study and that of achieved in the evaluation of Mwesigye and Meyer [34].

Besides, the PTC thermal efficiency is compared with the results of Mwesigye and Meyer [34]. In the study of Mwesigye and Meyer [34], a conventional PTC system is three dimensionally designed and simulated using ANSYS fluent software. The steady-state approach is used for simulating the PTC system and $k-\varepsilon$ is selected for modeling the working fluid in the tube. Moreover, the SIMPLE algorithm with second-order upwind schemes is used for solving the equations.

Fig. 4 (b) shows the variation of PTC thermal efficiency versus the operating fluid inlet temperature in the study of Mwesigye and the current assessment [34]. As illustrated, the obtained outcomes have a good accommodation. The greatest and average amount of error between the studies is about 3 % and 1.7 %, respectively. In conclusion, due to the good agreement between the data of the study of Mwesigye and Meyer and the current assessment [34], the numerical outputs of the present investigation are reliable enough.

5. Results

In the present research, the performance of all PTC-PV, PTC, PTC-ORC, and PTC-PV-ORC systems are evaluated from both exergy and energy viewpoints. In this regard, the ORC performance is studied, henceforth the effect of integration of this cycle with the PTC and PTC-PV unit is scrutinized. In the simulations, the working conditions of the systems are as same as the base case situation which is indicated in Table 3. As shown in this table, for evaluating the effect of solar flux intensity and concentration ratio every time one parameter is fixed and the other is variable.

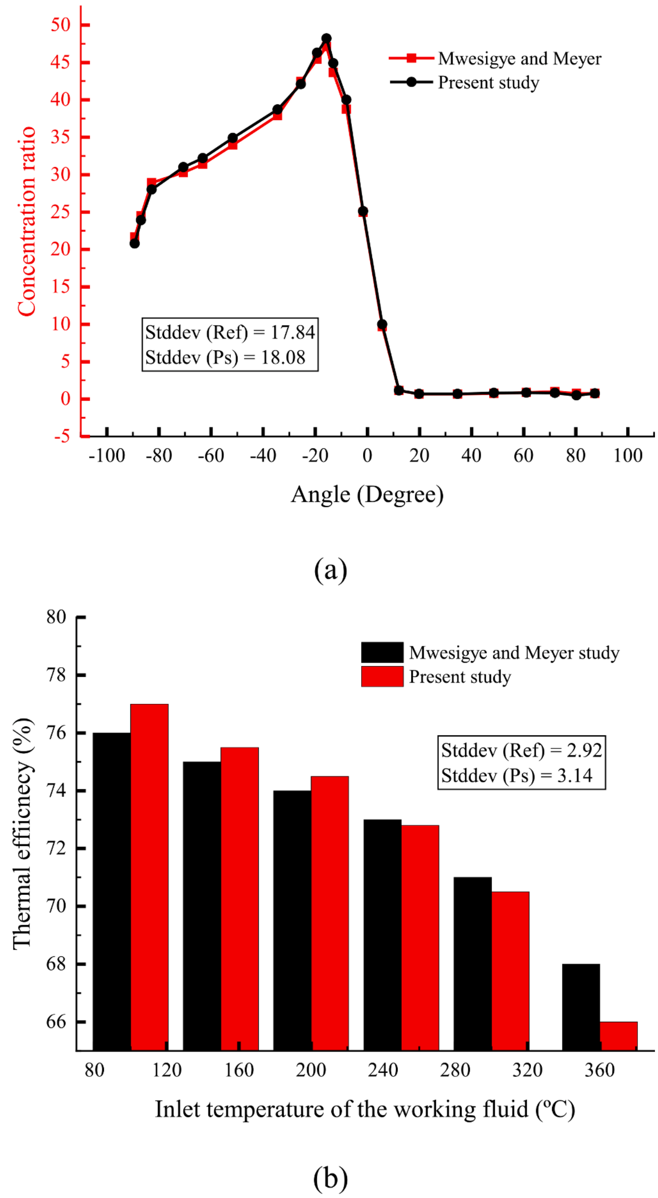

Fig. 4. Collation evaluation between the obtained outcomes of the study and corresponding data from Mwesigye and Meyer [34] (a) solar flux concentration and (b) thermal efficiency.

Table 3
Working condition of the PTC and PTC-PV systems.

Criteria	Base condition	Variation
Solar irradiance (W/m^2)	800	400–1200
Concentration ratio	35	25–45
Mass flow rate of operating fluid (kg/h)	360	–
Considered ambient temperature (°C)	30.1	–
Considered wind speed (m/s)	1	–

In Fig. 5, the efficiency of the ORC system and the inlet temperature of the condenser of the cycle versus the inlet temperature of the turbine is presented. It should be noted that the turbine inlet temperature is equal to the final temperature of the R407c when leaves the heat exchanger. As pictured in Fig. 5, increasing the turbine inlet temperature enhances both the thermodynamic performances of the proposed unit and the fluid inlet temperature when enters the condenser. Thus, the electrical and thermal energy performances of the mentioned unit boost.

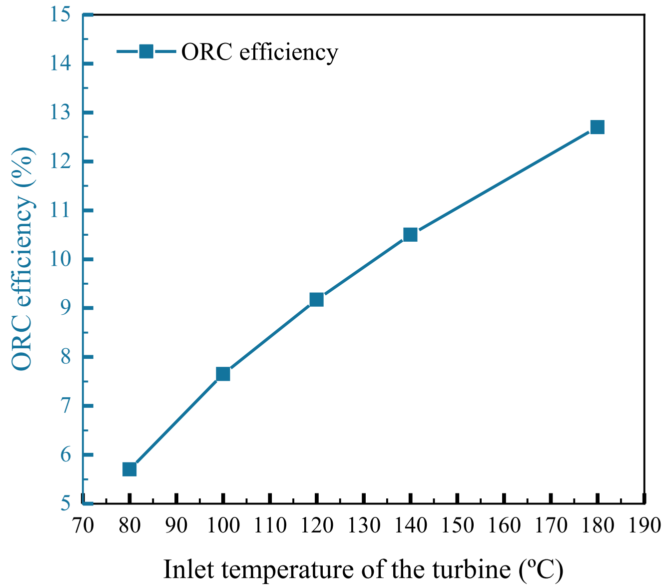

Fig. 5. The variation of ORC efficiency and condenser inlet temperature versus the inlet temperature of the ORC turbine.

The thermal, electrical, and overall energy efficiencies of the simulated systems are exhibited in Fig. 6. As shown in Fig. 6 (a), increasing solar flux from 400 W/m^2 to 1200 W/m^2 continuously declines the thermal energy efficiencies of both the PTC and PTC-PV systems. The thermal efficiencies of the PTC and PTC-PV systems at the solar flux of 400 W/m^2 are 43.17 % and 38.22 %, respectively. On the other hand, the thermal efficiencies of the PTC and PTC-PV systems at the solar flux of 1200 W/m^2 are 41.94 % and 37.04 %, respectively. The main reason for this phenomenon is the elevation in the rate of heat transfer from the tube to the ambient by raising solar flux.

In the PTC-ORC and PTC-PV-ORC systems, although increasing solar flux from 400 W/m^2 to 800 W/m^2 has an unfavorable impact on the thermal performances, ascending solar flux from 800 W/m^2 to 1200 W/m^2 boosts the thermal performance of the units.

The impacts of solar flux on the electrical generations of the systems are provided in Fig. 6 (b). This figure demonstrates that raising solar flux harms the electrical efficiencies of the PTC-ORC and PTC-PV-ORC systems. The electrical production of the PV module is highly dependent on the operating temperature of the solar cells. Raising the temperature of the cells intensely reduces the electrical energy generation of the module. Therefore, this decrement in the electrical performance of the PTC-ORC and PTC-PV-ORC systems can be justified due to the dependency of these systems on the electrical output of the solar cells. Nonetheless, the electrical performance of the PTC-ORC system is dependent only on the performance of the ORC unit.

In the PTC-ORC unit, raising solar flux causes an increment in the temperature of the operating fluid at the inlet of the turbine leading to higher electrical energy production. The electrical energy efficiency of the PTC-ORC unit is enhanced from 2.33 % to 4.72 % by increasing solar flux from 400 W/m^2 to 1200 W/m^2.

Based on Fig. 6 (c), raising solar flux declines the electrical performances of all systems except PTC-ORC. According to the results, the overall energy efficiencies of the conventional PTC, PTC-ORC, PTC-PV, and PTC-PV-ORC systems at the solar fluxes of 400 W/m^2 are 43.17 %, 33.82 %, 50.22 %, and 52.29 %, respectively. These values at the solar flux of 1200 W/m^2 are calculated to be 41.94 %, 17.81 %, 43.97 %, and 20.66 %, respectively. From the energy viewpoint, in the low solar flux, the PTC-PV-ORC system has the highest performance, while, in the high intensities, the PTC-PV system has the best output.

Fig. 7 demonstrates the thermal, electrical, and overall exergy efficiencies of the systems versus solar flux. As presented, the thermal

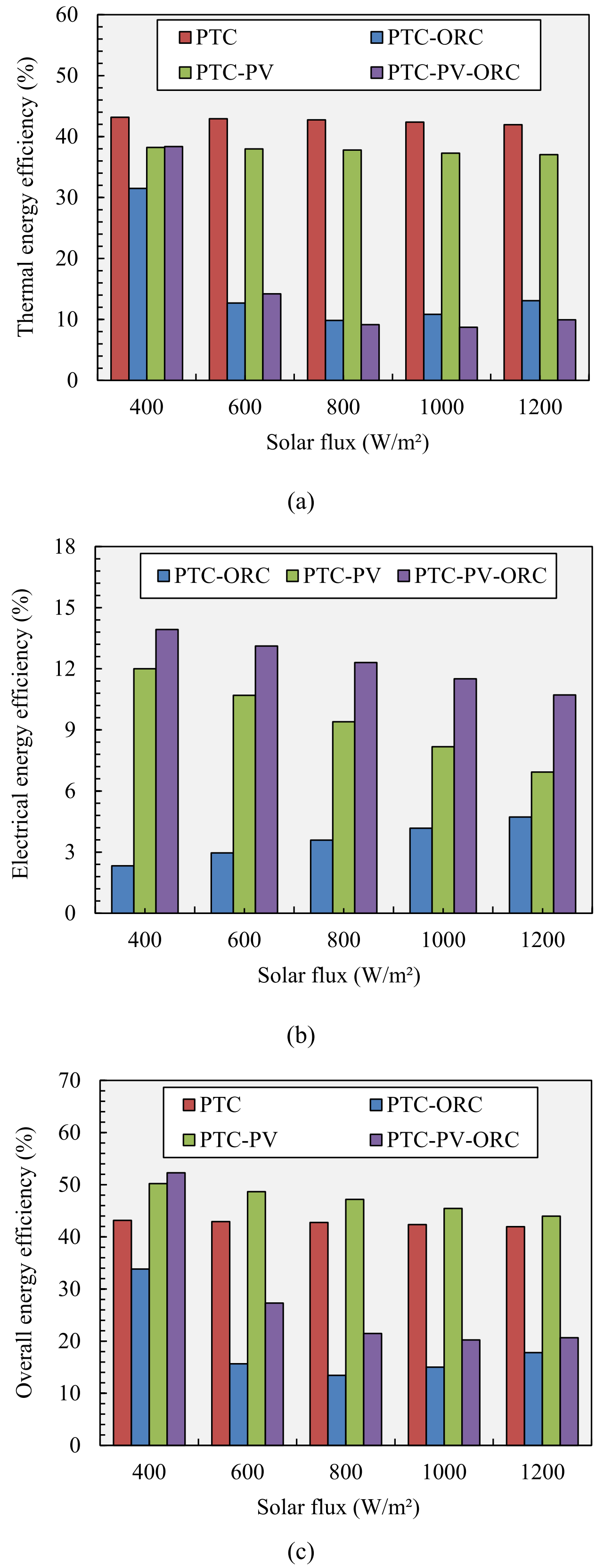

Fig. 6. (a) The thermal (b) electrical, and (b) overall energy efficiency of the systems versus solar flux.

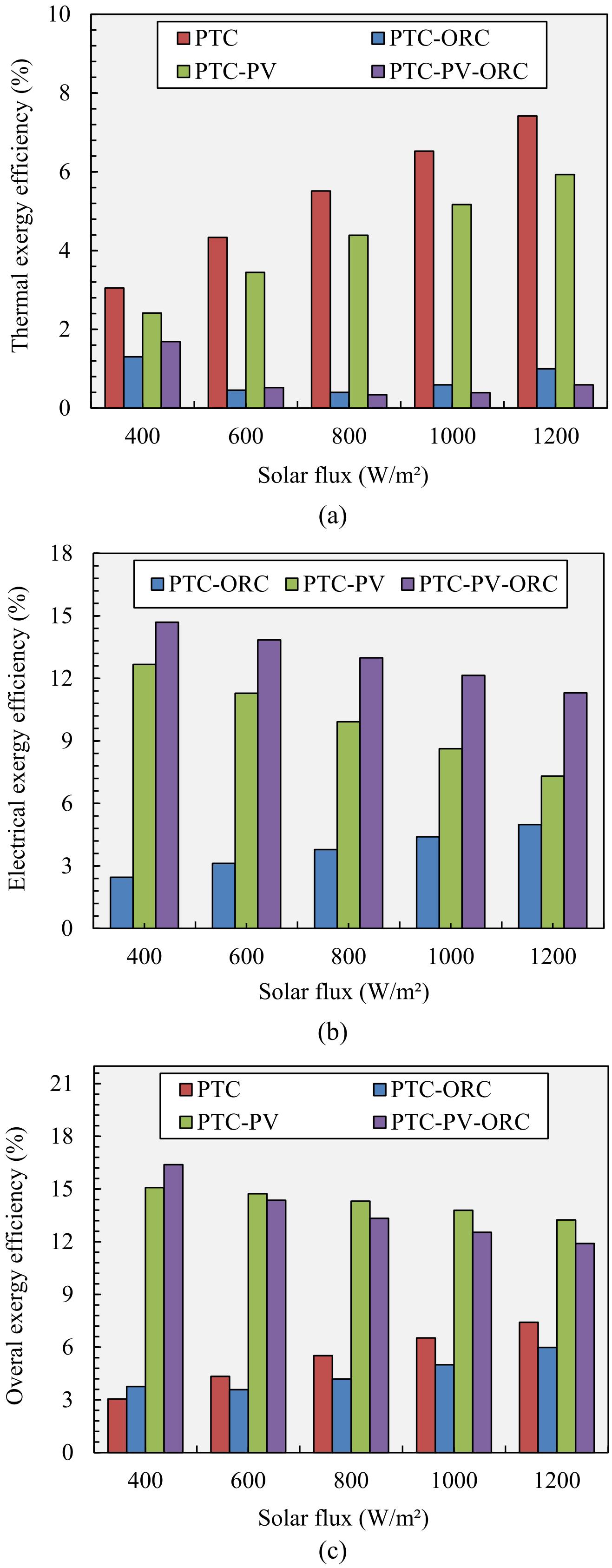

Fig. 7. (a) The thermal (b) electrical, and (b) overall exergy efficiency of the systems versus solar flux.

exergy performances of the PTC and PTC-PV units are superior to the ORC-based systems. In the systems coupled with ORC, a part of thermal energy converts to electrical power, and the remained heat is delivered to the ambient through the condenser at low temperatures leading to a reduction in the thermal exergy output of the units. The thermal exergy efficiencies of the conventional PTC, PTC-ORC, PTC-PV, and PTC-PV-ORC at the solar flux of 1200 W/m^2 are 7.42 % 1.00 %, 5.93 %, and 0.59 %, respectively. Besides, the electrical exergy performances of the systems are similar to those of electrical energy performances.

Furthermore, the computational outputs reveal that the overall exergy performances of the conventional PTC and PTC-PV systems are continuously enhanced by raising solar flux intensity. Nevertheless, elevation in the solar flux slightly declines the overall exergy output of the systems. In the solar flux of 400 W/m^2, the PTC-PV-ORC systems have the best performance followed by PTC-PV, PTC-ORC, and conventional PTC systems. However, in the solar flux of 1200 W/m^2, the PTC-PV has the highest efficiency followed by PTC-PV-ORC, conventional PTC, and PTC-ORC systems.

The temperature distributions in both PTC and PTC-PV systems at various solar fluxes are portrayed in Fig. 8. As indicated, both the outlet and absorber temperatures of the PTC system are more than that of the PTC-PV. In PV-based systems, a portion of the solar energy converts to electricity; thus, a lower amount of heat will shift from the absorber to the working fluid compared to the PTC unit.

Moreover, increasing solar flux intensity ascends the outlet temperature of the operating fluid which can be attributed to the higher heat transfer rate from the tube to the fluid. Additionally, the absorber temperature in the bottom sections is more than that of the upper areas. Non-uniform solar flux dispensation over the tube causes a non-uniform temperature distribution in the absorber. The reflector of the unit concentrates most of the solar rays on the absorber tube bottom section, while in the upper sections, the tube receives solar energy directly from the sky not the reflector of the system.

The influences of the concentration ratio on the energy performances of the simulated systems are depicted in Fig. 9. As provided, increasing concentration ratio from 25 to 45 reduces the thermal energy performances of the conventional PTC, PTC-ORC, PTC-PV, and PTC-PV-ORC systems from 45.04 % to 41.46 %, 13.33 % to 10.68 %, 40.44 % to 36.38 %, and 14.68 % to 8.53 %, respectively. The lower thermal energy performance of the ORC-based systems compared to the single solar power units is due to the thermal to electrical energy conversion by the turbine. Moreover, raising the concentration ratio on the surface of the tube increases the temperature of the receiver leading to higher heat transfer from the system to the ambient through both convection and radiation mechanisms. The PTC and PTC-PV systems have the highest performance among the simulated systems at various concentration ratios from the thermal energy viewpoint.

Furthermore, the results show that at all studied concentration ratios, the PTC-PV-ORC system outperforms among the systems. The electrical energy efficiencies of the PTC-ORC, PTC-PV, and PTC-PV-ORC systems are obtained to be 4.10 %, 8.15 %, and 11.41 %, respectively. Also, the impacts of variation in concentration ratio on the PV-based systems are much higher than that of ORC-based systems. It should be noted that the conventional PTC system is not able to provide any electrical energy.

The overall energy analysis of the systems reveals that the outputs of the single solar units are higher than those of units combined with the PV module. However, the main parts of the produced energies by the conventional PTC and PTC-PV systems are in the form of thermal energy.

Fig. 10 portrays the thermal, electrical, and overall exergy efficiencies of the systems. Based on Fig. 10 (a), the thermal exergy efficiencies of the ORC-based systems at multiple operating conditions are intensely lower than those of conventional PTC and PTC-PV systems. In the ORC-based systems, the thermal energy transfers from the solar section to the ORC. In the cycle, the hot fluid enters the turbine and

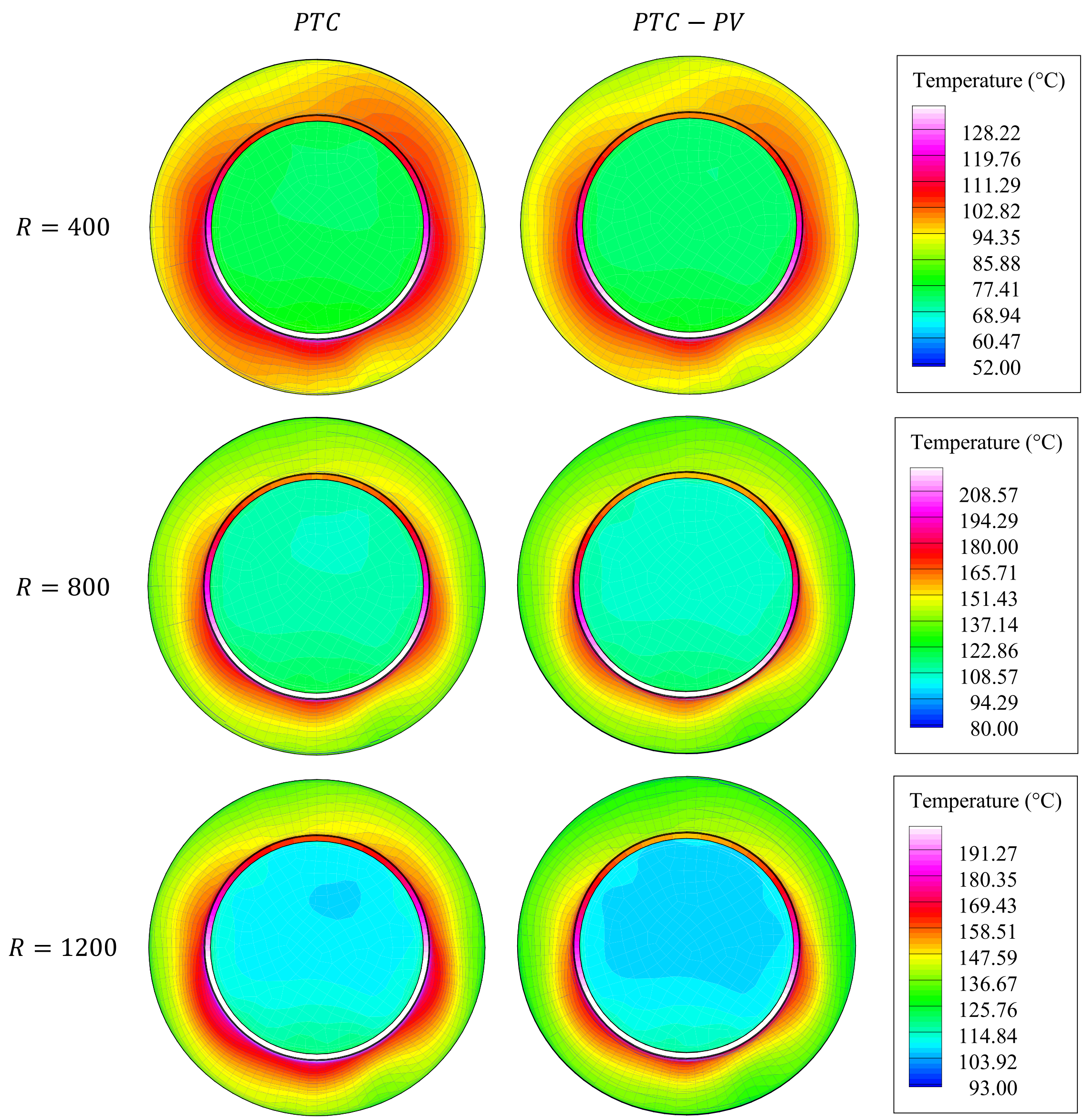

Fig. 8. The temperature distribution in the PTC and PTC-PV systems at different solar fluxs.

produces electrical energy. Afterwards, the fluid with low temperature enters the condenser and releases its remained heat to the cooling fluid. Hence, a limited thermal exergy is provided by these types of hybrid systems. The thermal exergy efficiencies of the conventional PTC, PTC-PV, PTC-ORC, and PTC-PV-ORC systems are 6.42 %, 5.06 %, 0.59 %, and 0.39 %, respectively. Moreover, the electrical exergy efficiencies presented in Fig. 10 (b) are similar to the electrical energy performances of the system (Fig. 9 (b)). The electrical exergy efficiencies of the PTC-ORC, PTC-PV, and PTC-PV-ORC systems are computed to be 4.33 %, 8.60 %, and 12.04 %, respectively.

Finally, the overall exergy efficiencies of the systems at multiple concentration ratios are depicted in Fig. 10 (c). Based on the findings, the overall exergy efficiencies of the conventional PTC and PTC-ORC systems are enhanced by raising the concentration ratio of the systems. Increasing the concentration ratio of the systems from 25 to 45 boosts the overall exergy efficiencies of the PTC and PTC-ORC systems from 4.55 % to 6.42 % and from 3.76 % to 4.92 %, respectively. Nevertheless, the ascending concentration ratio of the systems from 25 to 45 diminishes the overall exergy efficiencies of the PTC-PV and PTC-PV-ORC systems from 14.94 % to 13.66 % and from 14.51 % to 12.43 %, respectively.

Also, the temperature distribution on the symmetry line of both the PTC and PTC-PV systems at the receiver tube outlet is pictured in Fig. 11. As can be seen, all components of the PTC system have higher temperatures compared to the PTC-PV hybrid system. In both systems, the glass coating has the lowest temperature due to its interaction with the surrounding environment. Also, as mentioned earlier, the temperature of the absorber zone in the PTC-PV renewable unit is less than that of the PTC unit due to the energy conversion in this layer. Also, due to the lower heat transfer rate among the absorber layer and the working fluid in the hybrid PTC-PV generation unit, the fluid temperature in the PTC unit is more than the corresponding data of the PTC-PV unit, which can lead to lower thermal energy and exergy performances of the novel PTC-PV unit. But, due to the electricity production in the PV module, the overall performance of the PTC-PV unit is more than that of the PTC unit.

Although the integration of the PTC or PTC-PV system with the ORC reduces the net energy performance of the renewable unit, it enhances the exergy output of the coupled device, remarkably. Considering the simulation outcomes, the PTC-PV-ORC generation unit has the highest exergy performance among the studied systems.

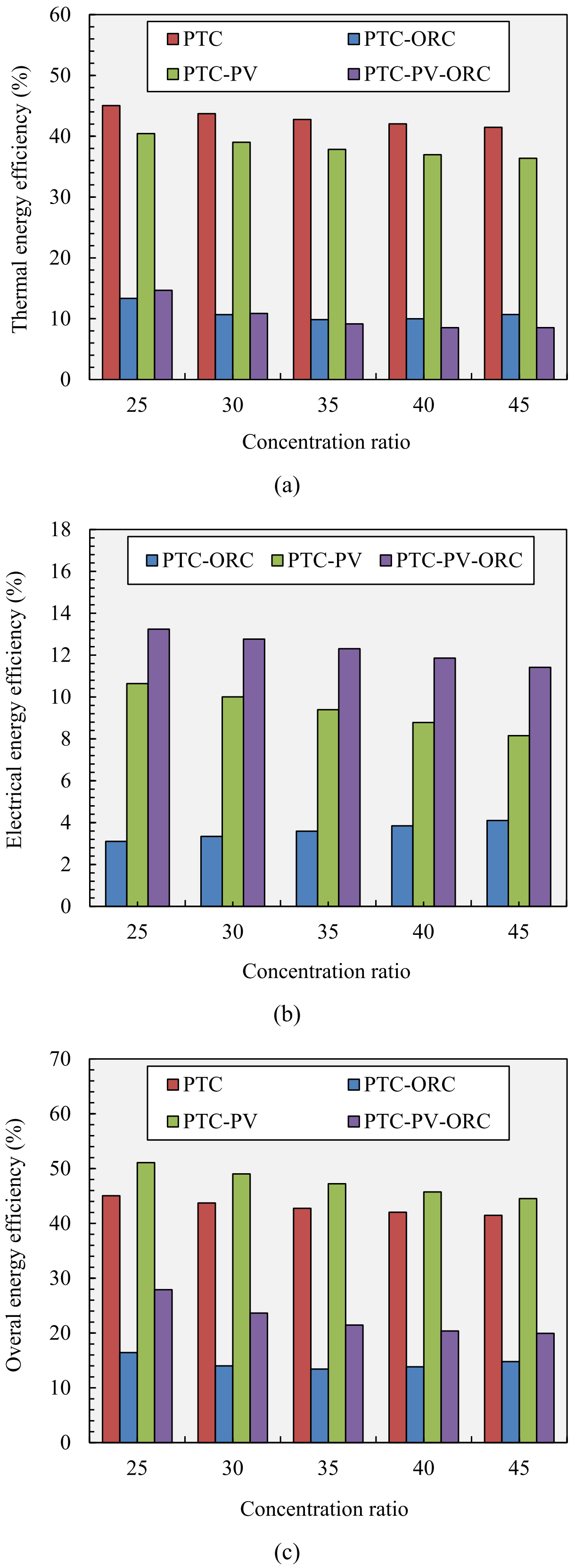

Fig. 9. (a) The thermal (b) electrical, and (b) overall energy efficiency of the systems versus concentration ratio.

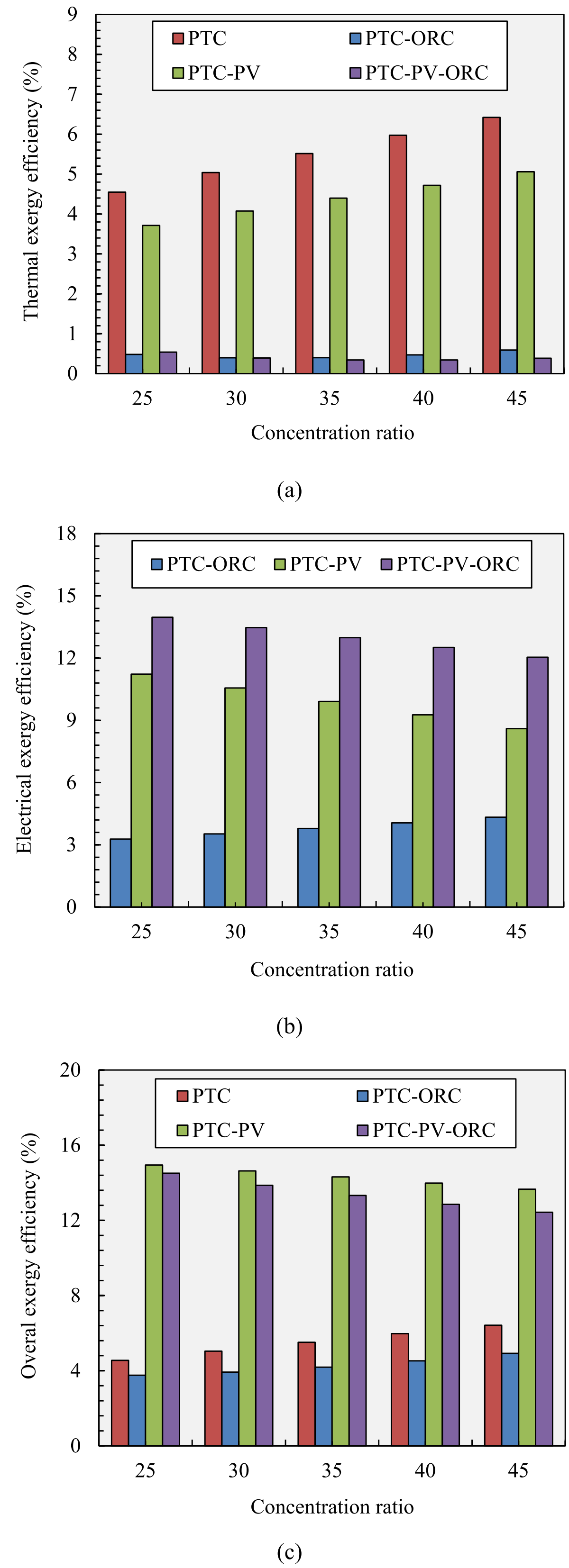

Fig. 10. (a) The thermal (b) electrical, and (b) overall exergy efficiency of the systems versus concentration ratio.

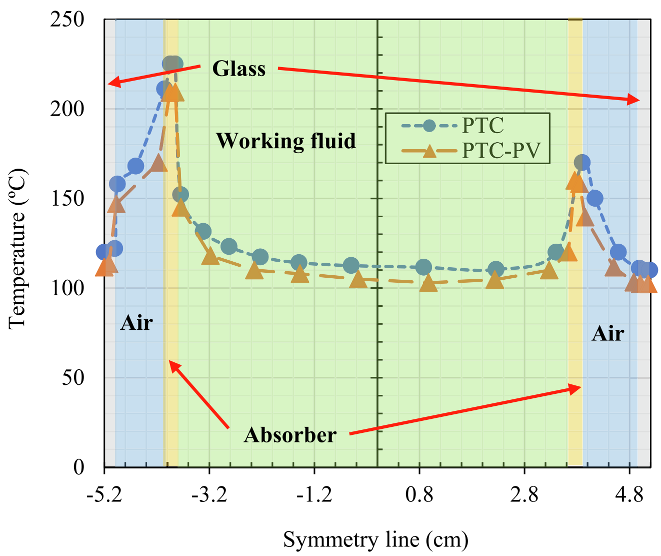

Fig. 11. The temperature dispensation on the symmetry line of both the PTC and PTC-PV system at the receiver tube outlet.

6. Conclusion

In this present research, the efficiencies of different hybrid parabolic trough solar collectors are evaluated from both the energy and exergy viewpoints. The solar unit is three-dimensionally designed and simulated using the steady-state approach. Also, the performance of the organic Rankine cycle is computed mathematically. In the coupled systems, the thermal energy of the solar unit is delivered to the cycle through a heat exchanger. In order to analyze the efficiencies of the systems, the designed units are simulated at various solar fluxes and concentrated ratios. The most substantial achievements of this paper are as follows:

- Integration of the parabolic trough solar collector with the cycle increases the net exergy output of the hybrid generation unit while it declines its overall energy performance.
- The PTC-PV and PTC-ORC hybrid systems have the highest and lowest performance from the energy viewpoint. Actually, in the low solar fluxes, the PTC-PV-ORC system has the highest energy performance among the studied systems, while in the high intensities, the PTC-PV system has the best energy performance.
- Nevertheless, from the exergy viewpoint, the PTC-PV system has the optimum performance followed by PTC-PV-ORC, conventional PTC, and PTC-ORC systems, respectively.
- The electrical energy and exergy analysis of the systems shows that the collector integrated with both solar cells and the cycle has the highest performance.
- Increasing the solar irradiance intensity and concentration ratio reduces the energy performance of the systems while raising the value of these parameters has a positive impact on the exergy efficiencies of both conventional solar units and collectors integrated with solar cells.

Based on current research, the combination of solar power systems with the cycle boosts the exergy efficiencies of renewable systems due to thermal to electrical energy conversion by the ORC. On the other hand, integrating the PTC with the PV module can enable the system to produce extra electrical energy in addition to thermal power. According to the findings, the PTC-PV-ORC system is the best option from the electrical energy production viewpoint. Nevertheless, when the overall performance is the priority, the PTC-PV system is the best option. This study proposed novel methods that can enhance the performance of conventional PTC unit.

Although this study takes a prominent step toward a deeper understanding of the performance of parabolic trough solar collectors, some topics can attract the attention of the researchers. In the following, some of the most interesting ideas are provided:

- Evaluating the effect of ORC configuration on the overall exergy and energy performances of the coupled unit.
- Assessment of the consequence of working fluid on the system performance.
- Evaluating the effect of using nanofluid-based PTC unit on operating of the coupled device.

Declaration of Competing Interest

The authors declare that they have no known competing financial interests or personal relationships that could have appeared to influence the work reported in this paper.

Data availability

Data will be made available on request.

Acknowledgments

- This work was funded by the National Natural Science Foundation of China (Grant Number 52150410418)
- The authors are grateful to the Researchers Supporting Project number (RSPD2023R669), King Saud University, Riyadh, Saudi Arabia, for the financial support.
- Authors acknowledge financial support from Abu Dhabi University's Office of Research and Sponsored Programs.

References

[1] K. Zhao, H. Jin, Z. Gai, H. Hong, A thermal efficiency-enhancing strategy of parabolic trough collector systems by cascadingly applying multiple solar selective-absorbing coatings, Appl. Energy 309 (2022) 118508.
[2] M.A. Hamada, H. Khalil, M. Abou Al-Sood, S.W. Sharshir, An experimental investigation of nanofluid, nanocoating, and energy storage materials on the performance of parabolic trough collector, Appl. Therm. Eng. 219 (2023) 119450.
[3] M.M. El-Bakry, M.A. Kassem, M.A. Hassan, Passive performance enhancement of parabolic trough solar concentrators using internal radiation heat shields, Renew. Energy 165 (2021) 52–66.
[4] K. Reddy, C. Ananthsornaraj, Design, development and performance investigation of solar Parabolic Trough Collector for large-scale solar power plants, Renew. Energy 146 (2020) 1943–1957.
[5] A. Salari, A. Taheri, A. Farzanehnia, M. Passandideh-fard, M. Sardarabadi, An updated review of the performance of nanofluid-based photovoltaic thermal systems from energy, exergy, economic, and environmental (4E) approaches, J. Clean. Prod. 282 (2021) 124318.
[6] M. Javidan, M. Gorji-Bandpy, A. Al-Araji, Investigation and simulation of parabolic trough collector with the presence of hybrid nanofluid in the finned receiver tube, Theor. Appl. Mech. Lett. 100465 (2023).
[7] M. Farooq, M. Farhan, G. Ahmad, M. Usman, M. Sultan, M.S. Hanif, M. Imran, S. Anwar, A.M. El-Sherbeeny, M.A. Shakir, Thermal performance enhancement of nanofluids based parabolic trough solar collector (NPTSC) for sustainable environment, Alex. Eng. J. 61 (2022) 8943–8953.
[8] S. Samiezadeh, R. Khodaverdian, M.H. Doranehgard, H. Chehrmonavari, Q. Xiong, CFD simulation of thermal performance of hybrid oil-Cu-Al2O3 nanofluid flowing through the porous receiver tube inside a finned parabolic trough solar collector, Sustainable Energy Technol. Assess. 50 (2022) 101888.
[9] N. Abed, I. Afgan, A. Cioncolini, H. Iacovides, A. Nasser, Effect of various multiple strip inserts and nanofluids on the thermal–hydraulic performances of parabolic trough collectors, Appl. Therm. Eng. 201 (2022) 117798.
[10] A. Aghaei, M. Enayati, N. Beigi, A. Ahmadi, H. Pourmohamadian, S. Sadeghi, A. Dezfulizadeh, A. Golzar, Comparison of the effect of using helical strips and fines on the efficiency and thermal–hydraulic performance of parabolic solar collectors, Sustainable Energy Technol. Assess. 52 (2022) 102254.
[11] Z. Esmaeili, S. Akbarzadeh, S. Rashidi, M.S. Valipour, Effects of hybrid nanofluids and turbulator on efficiency improvement of parabolic trough solar collectors, Eng. Anal. Bound. Elem. 148 (2023) 114–125.

[12] N.S. Reddy, S.G. Subramanya, K. Vishwanath, M. Karthikeyan, S. Kanchiraya, Enhancing the thermal efficiency of parabolic trough collector using rotary receiver tube, Sustainable Energy Technol. Assess. 51 (2022) 101941.

[13] S. Soltani, A. Kasaeian, T. Sokhansefat, M.B. Shafii, Performance investigation of a hybrid photovoltaic/thermoelectric system integrated with parabolic trough collector, Energ. Conver. Manage. 159 (2018) 371–380.

[14] A. Herez, H. El Hage, T. Lemenand, M. Ramadan, M. Khaled, Parabolic trough photovoltaic/thermal hybrid system: Thermal modeling and parametric analysis, Renew. Energy 165 (2021) 224–236.

[15] A. Padhy, B. Vishal, P. Verma, G. Dwivedi, A. Behura, Fabrication of parabolic trough hybrid solar PV-T collector using a-Si thin film solar cells in Indian perspective, Mater. Today:. Proc. 38 (2021) 56–62.

[16] D. Fu, G. Hu, M.K. Agrawal, F. Peng, B. Alotaibi, M. Abuhussain, T.R. Alsenani, Multi-criteria optimization of a renewable combined heat and power system using response surface methodology, Process Saf. Environ. Prot. 176 (2023) 898–917.

[17] Y.-Q. Feng, H.-J. Liang, K. Xu, Y. Wang, Y. Lu, C.-H. Lin, T.-C. Hung, Experimental study on the performance of a great progress 10 kW organic Rankine cycle for low-grade heat source based on scroll-type expander, Energy 284 (2023) 128627.

[18] F. Aziz, M.S. Salim, M.-H. Kim, Performance analysis of high temperature cascade organic Rankine cycle coupled with water heating system, Energy 170 (2019) 954–966.

[19] H. Habibi, M. Zoghi, A. Chitsaz, M. Shamsaiee, Thermo-economic performance evaluation and multi-objective optimization of a screw expander-based cascade Rankine cycle integrated with parabolic trough solar collector, Appl. Therm. Eng. 180 (2020) 115827.

[20] P. Pourmoghadam, M. Farighi, F. Pourfayaz, A. Kasaeian, Annual transient analysis of energetic, exergetic, and economic performances of solar cascade organic Rankine cycles integrated with PCM-based thermal energy storage systems, Case Studies in Thermal Engineering 28 (2021) 101388.

[21] M. Rostami, M.D. Manshadi, E. Afshari, Energy production and storage from a polygeneration system based on parabolic trough solar collector, proton exchange membrane fuel cell, organic Rankine cycle, and alkaline electrolyzer, J. Storage Mater. 47 (2022) 103635.

[22] S. Damarseckin, A. Atiz, M. Karakilcik, Solar pond integrated with parabolic trough solar collector for producing electricity and hydrogen, Int. J. Hydrogen Energy (2023).

[23] T. Wendelin Parabolic Trough VSHOT Optical Characterization in 2005-2006 (Presentation), in National Renewable Energy Lab.(NREL), Golden, CO (United States) 2006.

[24] H. Pierrick, M. Christophe, G. Leon, D. Patrick, Dynamic numerical model of a high efficiency PV–T collector integrated into a domestic hot water system, Sol. Energy 111 (2015) 68–81.

[25] J.J. Michael, I. Selvarasan, R. Goic, Fabrication, experimental study and testing of a novel photovoltaic module for photovoltaic thermal applications, Renew. Energy 90 (2016) 95–104.

[26] J.A. Duffie, W.A. Beckman, N. Blair, Solar Engineering of Thermal Processes, John Wiley & Sons, Photovoltaics and Wind, 2020.

[27] H. Singh, R. Mishra, Performance analysis of solar parabolic trough collectors driven combined supercritical CO2 and organic Rankine cycle, Engineering Science and Technology, an, Int. J. 21 (2018) 451–464.

[28] S. Mullick, S. Nanda, An improved technique for computing the heat loss factor of a tubular absorber, Sol. Energy 42 (1989) 1–7.

[29] W.C. Swinbank, Long-wave radiation from clear skies, Q. J. R. Meteorolog. Soc. 89 (1963) 339–348.

[30] A. Fluent Ansys fluent theory guide, Ansys Inc USA 15317 2011 724 746.

[31] M. Hosseinzadeh, A. Salari, M. Sardarabadi, M. Passandideh-Fard, Optimization and parametric analysis of a nanofluid based photovoltaic thermal system: 3D numerical model with experimental validation, Energ. Conver. Manage. 160 (2018) 93–108.

[32] H. Sun, J. Qin, T.-C. Hung, H. Huang, P. Yan, C.-H. Lin, Effect of flow losses in heat exchangers on the performance of organic Rankine cycle, Energy 172 (2019) 391–400.

[33] K. Braimakis, S. Karellas, Energetic optimization of regenerative Organic Rankine Cycle (ORC) configurations, Energ. Conver. Manage. 159 (2018) 353–370.

[34] A. Mwesigye, J.P. Meyer, Optimal thermal and thermodynamic performance of a solar parabolic trough receiver with different nanofluids and at different concentration ratios, Appl. Energy 193 (2017) 393–413.

[35] T.T. Chow, G. Pei, K. Fong, Z. Lin, A. Chan, J. Ji, Energy and exergy analysis of photovoltaic–thermal collector with and without glass cover, Appl. Energy 86 (2009) 310–316.

[36] D. Evans, Simplified method for predicting photovoltaic array output, Sol. Energy 27 (1981) 555–560.

[37] A.M. Norouzi, M. Siavashi, R. Ahmadi, M. Tahmasbi, Experimental study of a parabolic trough solar collector with rotating absorber tube, Renew. Energy 168 (2021) 734–749.

[38] S. Park, A. Pandey, V. Tyagi, S. Tyagi, Energy and exergy analysis of typical renewable energy systems, Renew. Sustain. Energy Rev. 30 (2014) 105–123.

[39] A. Kazemian, A. Salari, T. Ma, A year-round study of a photovoltaic thermal system integrated with phase change material in Shanghai using transient model, Energ. Conver. Manage. 210 (2020) 112657.